2013 European Control Conference (ECC)
July 17-19, 2013, Zürich, Switzerland.

Analysis of Vehicle Actuators Based on Reachable Sets

Balázs Németh and Péter Gáspár

Abstract— **The paper examines the reachability characteristics of vehicle actuators in order to analyse their abilities for the entire vehicle system. A computation method for an outer approximation of a reachable set is proposed. Simulation experiments are used in order to formulate the shape of the reachable sets of actuators. The evaluation of the shape provides preliminary information in the approximation of the reachable set. The upper bounds of the reachable set are calculated based on the constrained LMI feasibility problem in the nonlinear optimization task. The aim of the analysis is to provide a theoretical basis for the coordination of the actuators. The method is illustrated through the influence of the steering and the brake control systems at various velocities and road conditions.**

I. Introduction and motivation

Several active components are applied in road vehicles to solve different control tasks. In their simultaneous operation interference or conflict may occur in the entire vehicle system. The purpose of the integrated control is to take into consideration the effects of a control system on other vehicle functions, create coordination between controllers and provide priorities for actuators. In the integrated control there is a possibility to improve safety by modifying the operation of a local controller. If an actuator fault has occurred and it has been detected the faulty actuator is substituted for by another fault-free actuator which provides the same or similar control signal.

Recently, several important survey papers have been presented in this topic, see, e.g., [1], [2]. A vehicle control with four-wheel-distributed steering and four-wheel-distributed traction/braking systems is proposed by [3]. A process to design the control strategy for a vehicle with throttle control and automatic transmission is proposed by [4]. A yaw stability control system in which an active torque distribution and differential braking systems are used is proposed by [5]. An integrated control that involves both four-wheel steering and yaw moment control is proposed by [6]. Active steering and suspension controllers are also integrated to improve yaw and roll stability [7]. A global chassis control involving an active/semi-active suspension and brake is proposed by [8]. In integrated control systems the characteristics of the drivers' behavior are also taken into consideration in the control, see e.g. [9].

The authors are with Systems and Control Laboratory, Computer and Automation Research Institute, Hungarian Academy of Sciences, Kende u. 13-17, H-1111 Budapest, Hungary. E-mail: [bnemeth;gaspar] @sztaki.mta.hu

The research has been conducted as part of the project TÁMOP-4.2.2.A-11/1/KONV-2012-0012: Basic research for the development of hybrid and electric vehicles. The Project is supported by the Hungarian Government and co-financed by the European Social Fund.

The principles of the actuator selection are based on different factors, such as physical limits, energy requirements, effects and dynamics of the actuators, see [10]. Although the actuator selection is usually performed by using practical considerations, in the paper an analysis in which a theory-based approach is proposed is presented. The aim of the analysis is to identify the similarities and differences between the different actuator interventions.

In the proposed method the upper bounds of the reachable set are calculated based on the constrained LMI feasibility problem. In the nonlinear optimization task the results of simulation experiments are used. The reachability sets show the operation regions of the vehicle system. The sets show the similarities of the control systems, in which there is a possibility to substitute an actuator for another one. The sets show the differences between the control systems, in which an actuator may not be replaced by another one. In addition, these sets also identify the specialities of the actuators.

The paper is organized as follows: Section II formulates the bicycle model for the analysis of the reachability sets. An approximation of the reachable set is proposed in Section III. The steps of the algorithm are shown through an example of a vehicle model in Section IV. The analysis results of the reachable sets are also presented in this section. A reconfiguration control strategy based on the analysis results is presented in Section V. The applicability of the reachable set is illustrated through a simulation example in Section VI. Finally, the contributions of the paper are summarized in Section VII.

II. Modeling of vehicle lateral dynamics

The formulation of the vehicle lateral dynamics is based on the bicycle model, which is widely used in the control design of steering or braking, see [11]. In the first vehicle system the control signal is the differential brake moment M_{br}. The equations of vehicle lateral dynamics are the following:

$$\begin{aligned} J\ddot{\psi} &= C_1 l_1(-\beta - \dot{\psi} l_1/v) - C_2 l_2(-\beta + \dot{\psi} l_2/v) + M_{br} \\ mv(\dot{\psi} + \dot{\beta}) &= C_1(-\beta - \dot{\psi} l_1/v) + C_2(-\beta + \dot{\psi} l_2/v) \end{aligned} \quad (1)$$

where m is the mass, J is the yaw inertia of the vehicle and l_1 and l_2 are geometric parameters, C_1 and C_2 are cornering stiffnesses and v is longitudinal velocity. β is the side-slip and $\dot{\psi}$ is yaw-rate of the vehicle.

In the second vehicle system the control signal is the steering moment M_{st}. Besides the second-order bicycle model the formulation of steering dynamics considers steering resistances, such as the movement of the vehicle chassis and the gyroscopic effects of the steered wheels, which leads

to a second-order model of the steering system [10]:

$$J\ddot{\psi} = C_1 l_1(\delta - \beta - \dot{\psi} l_1/v) - C_2 l_2(-\beta + \dot{\psi} l_2/v)$$
$$mv(\dot{\psi} + \dot{\beta}) = C_1(\delta - \beta - \dot{\psi} l_1/v) + C_2(-\beta + \dot{\psi} l_2/v)$$
$$\vartheta\ddot{\delta} + \frac{2J_w v}{r_w}\dot{\delta} + B\pi s_{susp}(\sin n)\delta = M_{st} \quad (2)$$

where ϑ is the inertia of the wheel on the axle, J_w is the inertia of the wheel, r_w is the wheel radius, B is wheel track, s_{susp} is suspension stiffness and n is the angle between the road and the axle. δ is the front wheel steering angle.

Both models (1) and (2) depend on the velocity of the vehicle v nonlinearly and significantly. In the further analysis the velocity is chosen as a scheduling variable in the LPV (Linear Parameter Varying) model, i.e., $\rho = v$, which is valid for the entire velocity range. The state space representation in generic form is

$$\dot{x} = A(\rho)x + B(\rho)u \quad (3)$$

where the state vector of the system $x = \begin{bmatrix}\dot{\psi} & \beta\end{bmatrix}^T$ contains two state variables, i.e., the yaw rate $\dot{\psi}$ and the side-slip angle of the vehicle β. When the brake control is used the input of the system is $u = u_{br} = M_{br}$ and when the steering control is used the input is $u = u_{st} = M_{st}$.

In the paper the regions of the state variables are analyzed by calculating their reachability sets. In the calculations different inputs and road conditions are taken into consideration. The aim is to find the smallest outer approximation of the reachable sets of the LPV models.

III. Proposed method for the approximation of the reachable set

Several papers deal with reachable set computation, some of them are listed in the following. [12] introduces the ellipsoidal outer approximation of the reachable set for linear differential inclusion (LDI) systems. The set theoretic method is applied to design constrained $\mathcal{L}_2$ control and an algorithm is presented for the computation of the maximum disturbance invariant set in [13]. The reachable set method is applied in other areas of automotive research, see e.g. [14]. The reachable set computation method for LPV and quasi-LPV systems are proposed in [15]. Upper bounds for the reachable set and nonlinear system gains are characterized by polynomial Lyapunov functions in [16].

The reachable set of the vehicle systems are approximated by using ellipsoidal forms. According to the preliminary analysis the ellipsoid form is found as an appropriate selection. [12] presents the conditions to find the minimal reachable set for LDIs and linear systems. The LMI condition of the reachable set is formulated as:

$$\begin{bmatrix} A(\rho)^T P(\rho) + P(\rho)A(\rho) + \alpha P(\rho) + \dot{P}(\rho) & P(\rho)B(\rho) \\ B(\rho)^T P(\rho) & -\alpha I \end{bmatrix} \leq 0 \quad (4)$$

if there exists $P(\rho)$ and α satisfying $P(\rho) > 0$, $\alpha \geq 0$. The Lyapunov function of the system is chosen in a parameter-dependent way $V(x,\rho) = x^T P(\rho) x$, and time derivative of $P(\rho)$ is handled as $\dot{P}(\rho) = \frac{\partial P(\rho)}{\partial \rho}\dot{\rho}$. The upper limit of $\dot{\rho}$ is predefined as $\nu \geqq |\dot{\rho}|$ and $\frac{\partial P(\rho)}{\partial \rho}$ is computed using the formulation

$$P(\rho) = \sum_{i=1}^{N} f_i(\rho) P_i \qquad P_i \in \mathcal{R}^{nxn} \quad (5)$$

and f_i are appropriately-chosen basis functions. In the solution of the LMI feasibility problem it is necessary to find an α value in which $log(det(P(\rho)^{-1}))$ is minimal and which represents the volume over an ellipsoidal cylinder. In the proposed method the solution of (4) is the ellipsoidal approximation of the reachable set: $\varepsilon = \{x | x^T P(\rho) x \leq 1\}$.

According to our experience the computation of $P(\rho)$ may be numerically difficult because of the LMI condition (4). Moreover, the selection of f_i basis functions in (5) determines the qualification of reachable set approximation. However, the formulation of the basis function is not a trivial task.

In the paper a computation method for an outer approximation of the reachable set is proposed. Simulation experiments are used in order to formulate the shape of the reachable set. The evaluation of the shape provides preliminary information in the approximation of the reachable set.

The operations of the vehicle systems (1) and (2) are simulated by using a software, in which the model of the vehicle dynamics is represented with high accuracy. In this conception it is necessary to realize the suitable input signals, i.e., the steering moment and the brake yaw moment with their amplitudes and frequencies, which represent the vehicle dynamics in the entire range. Based on the appropriate simulation experiments, it is possible to analyze trajectories of the state variables $x = \begin{bmatrix}\dot{\psi} & \beta\end{bmatrix}^T$ in the function of velocity $\rho = v$. According to the visual information it is possible to identify their shapes and then provide a formulation of reachable set approximation which fits simulation results suitably. The trajectories help determine the structure of $P(\rho)$.

It must be verified whether $P(\rho)$ is the solution of LMI (4). The advantage of this method is that it is not necessary to solve the original LMI feasibility problem, because $P(\rho)$ is already known. If $P(\rho)$ represents the reachable set, then all of the eigenvalues of the following matrix are negative:

$$max\left(eig\left(\begin{bmatrix} A^T P + PA + \alpha P + \dot{P} & PB \\ B^T P & -\alpha I \end{bmatrix}\right)\right) < 0 \quad (6)$$

Note that (6) contains an $\alpha \geq 0$ parameter, which is not known in the computation of eigenvalues. In addition, $P(\rho)$ function contains some parameters μ_i, which are also not known. In the calculation of the reachable set it is necessary to find the smallest outer approximation. Thus, $P(\rho) = P(\rho, \mu_i)$ function must be optimized to provide the upper bound of the reachable set.

The optimization task is to find the solution

$$\min_{\mu_i, \alpha} \; log\left(det\left(P(\rho,\mu_i)^{-1}\right)\right), \quad (7)$$

while the constrains (6) and $\alpha \geq 0$ are fulfilled.

Using the proposed method the numerically complex LMI feasibility problem [12], [15] is replaced by a constrained optimization problem. There are several methods to solve the constrained optimization [17], [18]. The numerical solution is based on the Nelder-Mead simplex direct search algorithm, see [19]. The advantages of the replacement of LMI solution are that the original numerically difficult computation procedure is replaced by an easier solution and the complex nonlinear basis functions are substituted for using simulation experiments.

Remark 1: The simulation experiments have an important role in the approximation of the reachable set. However, it is necessary to emphasize that the proposed method always results in an outer approximation of the reachable set. The importance of the appropriate simulation is the evaluation of the shape of the reachable set. It helps formulate a suitable formulation of reachable set approximation.

IV. Simulation conditions and approximation of the reachable set

A. Reachable set approximation

The initial step of reachable set approximation is to create appropriate simulation examinations. In these simulations both the steering and the brake systems are analyzed and the input signals are selected in their entire amplitude and frequency range. Two kinds of signals are used as excitations, i.e., chirp (sinusoidal with linearly increasing frequency) and pulse signals. During simulations the velocity of the vehicle must also be changed because the nonlinear effect of velocity is analyzed. The velocity range is $50...100\ km/h$. The simulations are realized by using CarSim software, which is acceptable in the vehicle industry. The road condition is defined by an adhesion coefficient, which is within a narrow interval.

The formulation of the parameter-dependent Lyapunov function $P(\rho)$ is the following. The volume and the rotation of the elliptical cylinder change to the effect of velocity, therefore this information is used in the formulation of $P(\rho)$. The description of $P(\rho)$ is used in the approximation of the reachable set:

$$P(\rho) = T^T(\rho) P_0 T(\rho) \tag{8}$$

where P_0 is a level of the elliptical cylinder. $T(\rho)$ is a transformation matrix, which contains both volume and rotation:

$$T(\rho) = \left(1 + \mu_1 \left(\frac{\rho}{\rho_0} - 1\right)\right) \begin{bmatrix} \cos(\mu_2 \rho) & -\sin(\mu_2 \rho) \\ \sin(\mu_2 \rho) & \cos(\mu_2 \rho) \end{bmatrix} \tag{9}$$

where μ_1 and μ_2 are parameters and ρ_0 is the value of the scheduling variable at P_0 level.

The algorithm of the reachable set approximation is proposed in Section III. In optimization (6) and (7) it is necessary to compute the values of μ_1 and μ_2, which contain the information about the shape of the ellipsoidal cylinder. Figure 1 illustrates the approximation of the reachable set of the steering system, in which the simulation experiments are used. Red lines illustrate the result of the simulation experiments in the functions of the state variables β and $\dot{\psi}$ and the scheduling variable $\rho = v$, while blue ellipsoidal cylinders show the outer approximation of the reachable set. The ellipsoidal cylinders build the reachable set. The

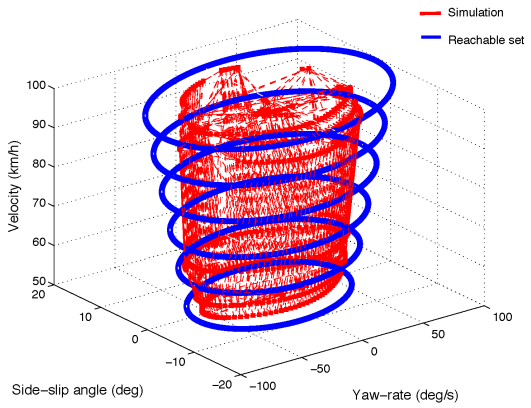

Fig. 1. Simulations and reachable set approximation

computation results show that ellipsoidal cylinders form an appropriate choice for this problem. The computed reachable set approximates the simulation results sufficiently, and fulfils (6) and (7).

B. Analysis of steering and braking reachable sets

In the following the preliminary results of the reachable set approximations are presented. The computation of the reachable sets is based on the proposed optimization method by using elliptical cylinders. The method requires simulation experiments. The model of the vehicle is represented with high accuracy by using CarSim/TruckSim software systems, which are acceptable in the vehicle industry. Different types of vehicles, road surfaces and velocities are used in the examinations. In the analysis a large family car ($1823\ kg$) with different adhesion coefficients is presented. They are $\mu_1 = 0.85$ (dry asphalt), $\mu_2 = 0.6$ (wet asphalt) and $\mu_3 = 0.4$ (wet and dirty asphalt or dirt-road). The influences of the steering moment and those of the differential brake yaw moment are analyzed.

Remark 2: In the simulation example the effect of adhesion coefficient μ on reachable sets is analyzed. However, there are other parameters which influence reachable sets during lateral dynamics, such as cornering stiffness values C_1, C_2. These parameters are handled as constant parameters in (1) and (2), but changes in their values may have an important role in actuator reachable sets. Parameters C_i, $i \in [1, 2]$ are expressed [11]:

$$C_i = \frac{\partial F_y}{\partial \alpha} = F_{zo} p_{Ky1} \sin\left(2 \arctan\left(\frac{F_z}{F_{zo} p_{Ky2}}\right)\right), \tag{10}$$

where F_{zo} is the nominal wheel load, F_z is the actual wheel load. andp_{Ky1} and p_{Ky2} are parameters, which depend on the tire-road contact, e.g. the adhesion coefficient, tire tread and wear. Consequently, other tire parameters also influence the tendency of reachable sets. It can be seen, however, that the most important factor of these parameters is the effect the

adhesion coefficient μ. This fact has motivated the analysis of μ in the example.

The first analysis focuses on the car. The approximation of the reachable sets is illustrated in Figure 2. The ellipsoidal cylinders show the outer approximation of the reachable sets in the functions of the state variables and the scheduling variable. Blue ellipsoids illustrate the influence of the braking system, while the yellow ellipsoids illustrate the influence of the steering system. The ellipsoidal cylinders build the reachable set. In the first analysis the effects of the road

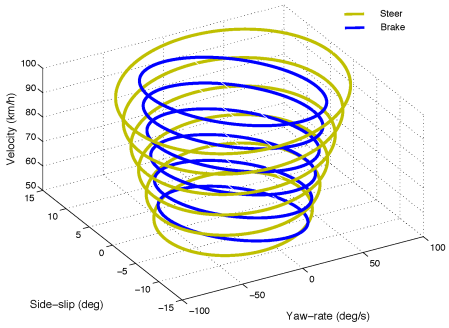

(a) $\mu = 0.85$

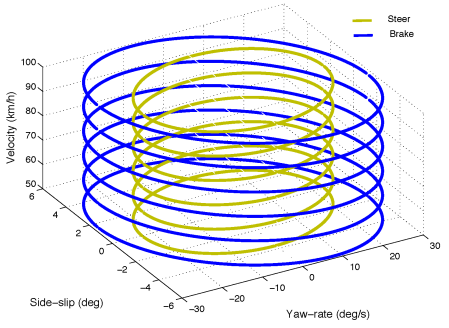

(b) $\mu = 0.6$

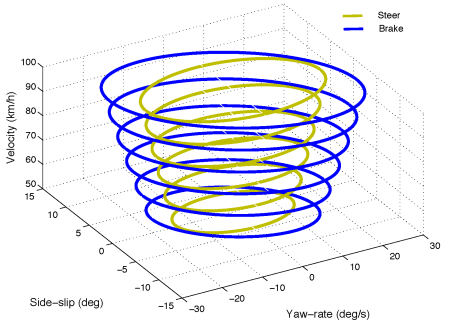

(c) $\mu = 0.4$

Fig. 2. Approximation of reachable sets in the case of car with different adhesion coefficients (blue: brake, yellow: steering)

conditions are compared, i.e., the effects of adhesion coefficients $\mu_1 = 0.85$, $\mu_2 = 0.6$, $\mu_3 = 0.4$ are illustrated in Figures 2(a), 2(b) and 2(c), respectively.

In excellent road (high μ) conditions the reachable set of the steering system is larger than the entire reachable set of the braking system according to both state variables in each scheduling variable. Consequently, the steering system should be used at high μ values, since it includes the reachable set of the brake system. However, at smaller adhesion coefficients the reachable set of the braking system is larger than that of the steering system. Both the volume and the rotation of elliptical cylinders change. In the case of wet or dirty asphalt the brake system is more effective than the steering. Consequently, the braking system should be used at smaller μ values, since it includes the reachable set of the steering system. The example shows that the adhesion coefficient and velocity have important role in the approximation of the reachable sets of the different actuators. Changes in the road adhesion coefficient and/or velocity require the interaction between the steering and the brake systems.

V. Control Strategy Based on Reachable Sets

In the following a reconfiguration control strategy based on the analysis results is presented. The aim of the control system is to avoid the lane departure of the vehicle. In the solution a reference yaw rate with an acceptable tracking error is predefined.

The reference yaw-rate signal is calculated by the following first-order reference system, which is represented by a transfer function from steering angle δ_d to reference yaw-rate signal $\dot{\psi}_{ref}$, see [20]:

$$G_{ref}(s) = \frac{v}{l_1 + l_2 + \frac{\eta}{g} v^2} \frac{1}{\tau s + 1} \tag{11}$$

where η is an understeer gradient [11], g is the gravitational constant and τ is the time constant. Consequently, the signal $\dot{\psi}_{ref}$ represents the driver's requirement. In the control design the purpose is to handle the tracking problem, i.e., the difference between $\dot{\psi}_{ref}$ and the actual yaw rate $\dot{\psi}$ must be minimized. The performance of the control system is

$$z = \dot{\psi}_{ref} - \dot{\psi}, \tag{12}$$

which guarantees the avoidance of lane departures.

The example in the previous section illustrates that there are states in the state space, which are not able to achieve by an actuator. However, these state may be reachable by another actuator of the vehicle. This is the basis of the reconfiguration of the control structure, in which the aim is to guarantee acceptable yaw-rate tracking during the journey. Figure 3 illustrates the reconfiguration strategy. The initial state vector of the system is x_0 and the reference state vector is $x_{ref} = [\dot{\psi}_{ref},\ \beta_{ref}]^T$, where $\dot{\psi}_{ref}$ is calculated by using (11) and β_{ref} is a parameter, which depends on vehicle dynamics and road conditions. It is assumed that actuator λ_1 provides a reachable set $\mathcal{R}_1$, which is illustrated by the solid blue ellipsoid. Since x_{ref} is outside from the reachable set of actuator λ_1, it is not achievable. However, actuator λ_2 is able to achieve x_{ref}, which is illustrated by the solid red ellipsoid $\mathcal{R}_2$. Thus, in order to achieve x_{ref} the reconfiguration from

actuator λ_1 to actuator λ_2 must be solved. Weights ρ_1 and ρ_2 are introduced for the selection of actuators λ_1 and λ_2, respectively, with the following constrains $0 \leq \rho_1, \rho_2 \leq 1$.

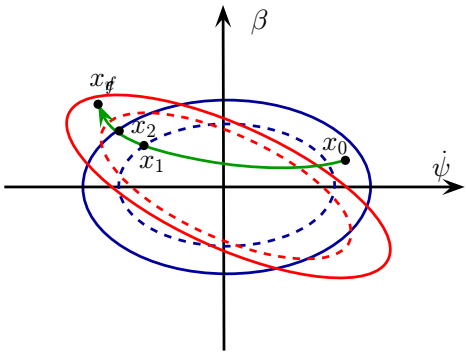

Fig. 3. Reconfiguration strategy

There are two other ellipsoids in Figure 3: the dashed blue ellipsoid $\mathcal{R}_{1d}$ is related to actuator λ_1 and dashed red ellipsoid $\mathcal{R}_{2d}$ is related to actuator λ_2. These ellipsoids are chosen to the borders of reachable sets as close as possible. Generally, the reconfiguration strategy is the following:

- If $(x_0 \;\&\; x_{ref}) \in \mathcal{R}_i$, the reachable set of actuator λ_i contains both the initial and reference states. Thus, x_{ref} can be achieved by the actuator λ_i without actuator reconfiguration. The actuator weights are selected $\rho_i = 1$ and $\rho_j = 0$.
- If $x_0 \in \mathcal{R}_i$ and $x_{ref} \in \mathcal{R}_j$, the reachable set of actuator λ_i is not able to achieve x_{ref}. Since actuator λ_j is able to achieve x_{ref} a reconfiguration between actuators is needed. The abrupt activation of actuators may results in large transients, which may degrade the performance properties of the vehicle. The state trajectory of the system is illustrated by the the green line in Figure 3. In terms of the state x_1 the trajectory achieves the border of $\mathcal{R}_{1d}$, therefore actuation of λ_1 must be reduced and actuation of λ_2 must be increased. In state x_2, which is at the border of $\mathcal{R}_1$ the operation of λ_1 is stopped and only actuator λ_2 works since $\mathcal{R}_2$ contains x_{ref}. In this way the abrupt activation of actuators should be avoided. The transition between λ_1 and λ_2 in a given x_k is defined by the following weights

$$\rho_1 = \frac{|x_{k,2}| - |x_k|}{|x_{k,2}| - |x_{k,1}|} \tag{13a}$$

$$\rho_2 = 1 - \rho_1 \tag{13b}$$

  where $x_{k,1}$ and $x_{k,2}$ are determined by the actual state x_k. Note that since the value x_2 is unknown when the actual state is x_k, an estimation of $x_{k,2}$ is needed, see Figure 4. The estimation can be solved by using an observer.
- If $x_{ref} \notin (\mathcal{R}_i \cup \mathcal{R}_j)$, the available actuators are not able to achieve the reference state. In this case the previous reference signal $\dot{\psi}_{ref}$ must be followed until the reference state is within the reachable sets.

In [21] a supervisory control design method, which integrates both the steering control K_{st} and the differential braking

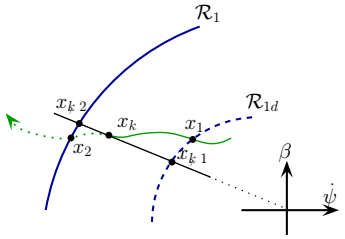

Fig. 4. Illustration of the actuator reconfiguration

control K_{br}, is presented. Applying parameter-dependent weighting functions coordination and priorities between different controllers are achieved. The reconfiguration is provided by weighting parameters ρ_{st} and ρ_{br}:

$$K_{st} = K_{st}(\rho_{st}) \tag{14a}$$

$$K_{br} = K_{br}(\rho_{br}) \tag{14b}$$

The weighting parameters are determined by the proposed reconfiguration strategy. The strategy requires look-up tables, which contains the results of the analysis of steering and braking reachable sets. During the journey the actuator selection requires four signals: they are the side-slip angle β, adhesion coefficient μ, yaw-rate $\dot{\psi}$ and velocity v in order to select the actual reachable set from the table. In practice, v and $\dot{\psi}$ are measured signals, μ is estimated by the algorithm [22], while β must be estimated on-line by using an observer.

VI. Simulation Results

The applicability of the reachable set is illustrated based on the operation of a supervisory control through a simulation example. In the example the CarSim software is used in order to represent the vehicle dynamics with high accuracy. The maneuvers of the driver along a course are assisted by the integrated control, which uses both steering angle and differential brake moment. It is assumed that road frictions and velocities change along the route.

Figure 5(a) shows the course of the vehicle, while Figure 5(b) and Figure 5(c) show the changes of the velocity and the adhesion coefficient, respectively. The bends in the course are hazardous from the aspect of lane departure. The actuator selection weights ρ_{st} and ρ_{br} are shown in Figure 5(d). The steering system is activated mainly in the first and last sections of the road, while in the middle sections differential braking is dominant. This actuator selection is based on the velocity, the adhesion coefficient and the reachable sets. Figure 2 shows that using the steering system at high μ it is possible to achieve an increased state space compared to the reachable set of the brake system. In the first and last sections of the road the tire-road friction is high, while in the middle sections it is low. In a section with low μ the brake system has a higher reachable set, therefore in the middle sections the brake is preferred.

The results of the control system are compared to the car without a driver assistance system. Both the yaw-rate error and the lateral error of the uncontrolled vehicle are extremely high, see Figure 5(e) and Figure 5(f). In this case the vehicle

leaves the road. In these figures the time responses of the control system are also shown. The control system is able to guarantee lane departure avoidance, since both the yaw-rate error and the lateral error are acceptable. Figure 5(g) and Figure 5(h) show both the steering angle and the differential brake moment of the control system.

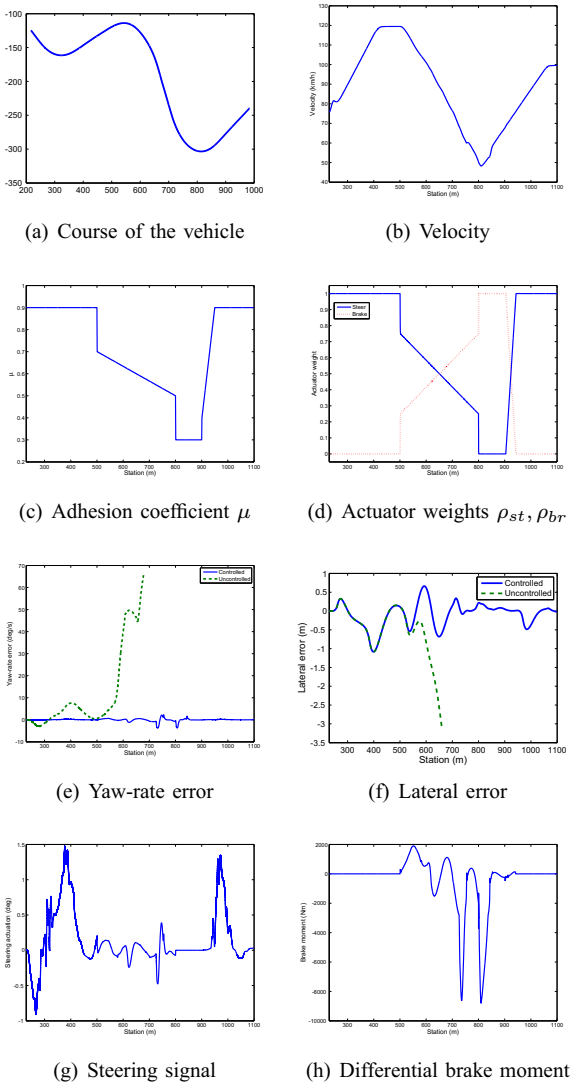

(a) Course of the vehicle (b) Velocity

(c) Adhesion coefficient μ (d) Actuator weights ρ_{st}, ρ_{br}

(e) Yaw-rate error (f) Lateral error

(g) Steering signal (h) Differential brake moment

Fig. 5. Time responses of vehicle maneuvers

VII. Conclusions

The paper has proposed a computation method for an outer approximation of a reachable set. Simulation experiments are used in order to formulate the shape of the reachable set. The evaluation of the shape provides preliminary information in the approximation of the reachable set. The calculation of the upper bounds of the reachable set is based on the constrained LMI feasibility problem in the nonlinear optimization task.

The reachable sets of different actuators show the similarities and differences between their interventions. The analysis shows that changes in important factors during maneuvers require the integration or reconfiguration of control components. The analysis provides information for an established theory whose aims is to coordinate the actuator interventions.

The simulation example has illustrated the efficiency of the driver assistance system. Based on the reachable sets the reconfigurable control system is able to handle different road conditions and velocities.

References

[1] F. Yu, D. Li, and D. Crolla, "Integrated vehicle dynamics control: State-of-the art review," *IEEE Vehicle Power and Propulsion Conference, Harbin, China*, 2008.

[2] P. Gáspár, Z. Szabó, and J. Bokor, "LPV design of reconfigurable and integrated control for road vehicles," *50th Conference on Decision and Control, Orlando*, 2011.

[3] E. Ono, Y. Hattori, Y. Muragishi, and K. Koibuchi, "Vehicle dynamics integrated control for four-wheel-distributed steering and four-wheel-distributed traction/braking systems," *Vehicle System Dynamics*, vol. 44, no. 2.

[4] D. Kim, H. Peng, S. Bai, and J. Maguire, "Control of integrated powertrain with electronic throttle and automatic transmission," *IEEE Trans. Control Systems Technology*, vol. 15:3, pp. 474–482, 2007.

[5] S. Zhang, T. Zhang, and S. Zhou, "Vehicle stability control strategy based on active torque distribution and differential braking," *Int. Conf. on Measuring Technology and Mechatronics Automation*, 2009.

[6] W. Jianyong, T. Houjun, L. Shaoyuan, and F. Wan, "Improvement of vehicle handling and stability by integrated control of four wheel steering and direct yaw moment," *Proc. 26th Chinese Control Conference, Zhangjiajie*, 2007.

[7] G. Mastinu, E. Babbel, P. Lugner, and D. Margolis, "Integrated controls of lateral vehicle dynamics," *Vehicle System Dynamics*, vol. 23, pp. 358–377, 1994.

[8] C. Poussot-Vassal, O. Sename, L. Dugard, P. Gáspár, Z. Szabó, and J. Bokor, "A new semi-active suspension control strategy through LPV technique," *Control Engineering Practice*, 2008.

[9] J. Lu and D. Filev, "Multi-loop interactive control motivated by driver-in-the-loop vehicle dynamics controls: The framework," *Joint 48th IEEE Conference on Decision and Control and 28th Chinese Control Conference, Shanghai*, 2009.

[10] B. Németh and P. Gáspár, "Design of actuator interventions in the trajectory tracking for road vehicles," *Proc. of the Conference on Decision and Control, Orlando, Florida*, 2011.

[11] H. B. Pacejka, *Tyre and vehicle dynamics*. Oxford: Elsevier Butterworth-Heinemann, 2004.

[12] S. Boyd, L. E. Ghaoui, E. Feron, and V. Balakrishnan, *Linear Matrix Inequalities in System and Control Theory*. Philadelphia: Society for Industrial and Applied Mathematics, 1997.

[13] T. Péni, B. Kulcsár, and J. Bokor, "Induced $\mathcal{L}_2$ norm improvement by interpolating controllers for discrete-time LPV systems," *European Journal of Control*, 2008.

[14] M. Althoff, O. Stursberg, and M. Buss, "Safety assessment of driving behavior in multi-lane traffic for autonomous vehicles," *IEEE Intelligent Vehicles Symposium*, pp. 893 – 900, 2009.

[15] J. Shin, "Analysis of linear parameter varying system models based on reachable sets," *American Control Conference, Anchorage*, vol. 1, pp. 35–40, 2002.

[16] W. Tan, U. Topcu, P. Seiler, G. Balas, and A. Packard, "Simulation-aided reachability and local gain analysis for nonlinear dynamical systems," *47th IEEE Conf. on Decision and Control, Cancun*, 2008.

[17] P. E. Gill, W. Murray, and M. Wright, *Practical Optimization*. Academic Press, London UK, 1981.

[18] R. Byrd, J. C. Gilbert, and J. Nocedal, "A trust region method based on interior point techniques for nonlinear programming," *Mathematical Programming*, vol. 89, no. 1, pp. 149–185, 2000.

[19] J. Lagarias, J. A. Reeds, M. H. Wright, and P. E. Wright, "Convergence properties of the nelder-mead simplex method in low dimensions," *SIAM Journal of Optimization*, vol. 9, no. 1, pp. 112–147, 1998.

[20] R. Rajamani, "Vehicle dynamics and control," *Springer*, 2005.

[21] P. Gáspár, B. Németh, and J. Bokor, "Design of an integrated control for driver assistance systems based on LPV methods," *Proc. of the American Control Conference , Montréal, Canada*, 2012.

[22] F. Gustafsson, "Slip-based tire-road friction estimation," *Automatica*, vol. 33, pp. 1087–1099, 1997.